GANP-mediated Recruitment of Activation-induced Cytidine Deaminase to Cell Nuclei and to Immunoglobulin Variable Region DNA*[S]

Kazuhiko Maeda[‡1], Shailendra Kumar Singh[‡], Kazufumi Eda[‡], Masahiro Kitabatake[‡], Phuong Pham[§], Myron F. Goodman[§], and Nobuo Sakaguchi[‡2]

From the ‡Department of Immunology, Graduate School of Life Sciences, Kumamoto University, 1-1-1 Honjo, Kumamoto 860-8556, Japan and the §Departments of Biological Sciences and Chemistry, University of Southern California, Los Angeles, California 90089-2910

AID (activation-induced cytidine deaminase) catalyzes transcription-dependent deamination of C → U in immunoglobulin variable (IgV) regions to initiate somatic hypermutation (SHM) in germinal center B-cells. SHM is essential in generating high affinity antibodies. Here we show that when coexpressed with GANP (germinal center-associated nuclear protein) in COS-7 cells, AID is transported from the cytoplasm and concentrated in the nucleus. GANP forms a complex with AID in cotransfected cells *in vivo* and *in vitro*. We have isolated AID mutants that bind with reduced affinity to GANP compared with wild type AID. One of these mutants, AID (D143A) binds GANP with a 10-fold lower affinity compared with wild type AID yet retains substantial C-deamination activity *in vitro*. Mutant AID (D143A) remains localized predominantly in the cytoplasm when coexpressed with GANP. Exogenous expression of GANP in Ramos B-cells promotes binding of AID to IgV DNA and mRNA and increases SHM frequency. These data suggest that GANP may serve as an essential link required to transport AID to B-cell nuclei and to target AID to actively transcribed IgV regions.

Affinity maturation of the humoral response proceeds by diversification of Ig genes (1, 2). Diversification requires AID[3]-initiated somatic hypermutation (SHM) within IgV regions and concomitant class switch recombination in Ig switch regions (S regions) (3). AID initiates SHM and class switch recombination by deaminating deoxycytidine residues during transcription of the Ig locus (4, 5). AID deaminates dC → dU on single-stranded DNA (ssDNA) and during the transcription of double-stranded DNA (6–8), presumably on the non-transcribed strand. AID favors deamination in WRC (where W represents A/T, and R is A/G) hot spot motifs (7). The observation of strongly enhanced C → T mutations in variable regions and S regions, which conform to the mutational signature of AID (7), offers convincing evidence that AID is acting directly on the transcribed DNA.

AID is located predominantly in the cytoplasm of activated B-cells (9) and has a nuclear localization signal motif in its N-terminal region and a nuclear export signal at its C terminus (10–12). Deletion of the nuclear export signal results in nuclear accumulation (11, 12) but does not result in an increase in mutations in S regions (11). There must be a means to regulate the import of AID into the nucleus and then to direct its access to transcribed Ig loci. Presumably, AID is recruited to specific Ig regions by a variety of targeting mechanisms that could include *cis*-acting transcription factors, proteins that associate with AID, and regions of ssDNA formed by transcription bubbles (4, 5). There are coimmunoprecipitation (co-IP) data showing interactions between AID and potential recruiter molecules, including RNA polymerase II (13), a spliceosome-associated factor CTNNBL-1 (14), ssDNA-binding protein (RPA) (8, 15), and protein kinase A (16). However, it remains unclear how AID is targeted preferentially to actively transcribed Ig genes; nor is it understood how AID is inhibited from deaminating non-Ig transcribed genes (17).

GANP is induced in GC B-cells during the immune response (18–20). It contains a region homologous to *Saccharomyces cerevisiae* SAC3 (21, 22), which is associated with the THO ribonucleoprotein complex involved in RNA export from the nucleus to the cytoplasm after transcription (23). GANP possesses two consensus signals, a nuclear localization signal (18), and two nuclear export signals (24), suggesting a potential shuttling movement between the nucleus and the cytoplasm. Mice lacking the *ganp* gene in B-cells fail to produce high affinity antibodies (Abs) against T-cell-dependent antigen (Ag) (20), whereas *ganp*-transgenic (*ganp^Tg*) mice exhibit an enhanced high affinity Ab production (25), demonstrating an essential

[3] The abbreviations used are: AID, activation-induced deaminase; SHM, somatic hypermutation; Ab, antibody; IgV, Ig variable; S, switch region; HIV, human immunodeficiency virus; IP, immunoprecipitation; anti-AID (M), anti-AID (mouse); Ag, antigen; nt, nucleotide(s); ChIP, chromatin immunoprecipitation; GC, germinal center; WT, wild type; ssDNA, single-stranded DNA; mAb, monoclonal antibody; qPCR, quantitative PCR; GFP, green fluorescent protein; WGE, wheat germ extract.

role for GANP in generating high affinity Abs in response to T-cell-dependent Ags (20). In this paper, we have performed experiments revealing that GANP may play a dual role in B-cell IgV diversification, first by localizing AID in the nucleus and second by helping to target AID to transcribed IgV region DNA.

EXPERIMENTAL PROCEDURES

Construction of Mammalian Expression Vectors—Mammalian expression vectors were constructed as follows. The *AcGFP* gene cassette from pAcGFP1 vector (Clontech) and *DsRed* gene cassette from pDsRed-Monomer vector (Clontech) were cloned into the XhoI site of pCXN2 vector carrying chicken *β-actin* promoter, resulting in constructs pCXN2-GFP and pCXN2-DsRed. The *hsp25* was amplified with 5′-GGGC-TCGAGTTACCATGACCGAGCGCCGCGTGCC-3′ and 5′-ACCGGATCCTTGGCTCCAGACTGT-3′. Mouse *ganp*, *aid*, and *hsp25* cDNAs were amplified by PCR inserted into the XhoI site of pCXN2-GFP and pCXN2-DsRed, giving expression vectors for fusion proteins, GFP-GANP, AID-DsRed, and HSP25-DsRed, respectively. All of the constructs were verified by sequencing on both strands.

Construction of in Vitro Expression Vectors—FLAG-tagged GANP (encoding the region from amino acid 148 to l,919) and the N-terminal HA-tagged AID were amplified by PCR and cloned into the pTNT® vector (Promega). A mutation (D143A) in the vector encoding *aicda* cDNA was generated with the QuikChange® II XL site-directed mutagenesis kit (Stratagene). The oligonucleotide used together with its complementary sequences was as follows: 5′-GGGATCATGACCTTC-AAAGCCTATTTTTACTGCTGGAAT-3′.

Cell Culture and cDNA Transfection—COS-7 and human Burkitt lymphoma cell line Ramos cells were maintained in Dulbecco's modified Eagle's medium and RPMI 1640 medium supplemented with 10% heat-inactivated fetal bovine serum, respectively. For immunofluorescence analysis, COS-7 cells (1×10^6 cells) were mixed with each expression vector (1.5 μg for GFP alone and DsRed fusion proteins, 4.5 μg for GFP-GANP) and transfected by using Amaxa's Nucleofection kit R^{TM} (program O-01) according to the manufacturer's protocols. For coimmunoprecipitation assay, transfection was performed using FuGENE® HD transfection reagent (Roche Applied Science) according to the manufacturer's protocols. For the RNA/DNA-ChIP assay, Ramos cells (1×10^7 cells) were transfected with 30 μg of GFP expression vector or 60 μg of GFP-GANP expression vector by electroporation (Gene Pulser Xcell^{TM}, Bio-Rad) in a 0.4-cm cuvette with a voltage of 280 V/cm and capacitance of 975 microfarads.

Immunoprecipitation and Western Blotting—The COS-7 transfectants were lysed in TNE buffer (10 mM Tris-HCl, pH 7.5, 150 mM NaCl, 1 mM EDTA, 1% Nonidet P-40 (Nonidet P-40)) containing the protease inhibitor mixture (Nacalai Tesque). To digest the RNA or DNA, the cell lysate was preincubated with either 250 μg/ml RNase A (Nippongene) or 50 units of Turbo DNase I (Ambion) for 10 min. Immunoprecipitation was carried out by incubating the cell lysates with GFP, AID, or β-actin Ab in the presence of protein A/G-agarose (GE Healthcare). After washing the immunoprecipitates (six times) with TNE buffer, the pellets were resuspended in Laemmli

SDS-sample buffer, boiled, separated on the gradient SDS-polyacrylamide gel, and transferred to nitrocellulose membrane (Bio-Rad). Western blots were developed by appropriate primary Ab and a secondary Ab conjugated to horseradish peroxidase using Immobilon Western reagent (Millipore), and protein bands were visualized by the VersaDoc system (Bio-Rad).

Expression and Purification of Recombinant Proteins—Recombinant proteins for the cell-free assay were prepared by a wheat germ extract (WGE)-based cell-free protein synthesis kit, the TNT® SP6 high yield system (Promega), according to the manufacturer's protocol. For *in vitro* binding assay, each 2 μl of WGE was mixed in TNE buffer and precipitated with anti-FLAG Ab.

Mutant AID Purification and Activity Assay—Recombinant wild type and mutant AID (D143A) proteins were expressed in baculovirus-infected *Sf*9 cells and purified as described previously (6, 7). C→U deamination activity of WT and mutant AID were assayed using ^{32}P-labeled 36-nucleotide (nt) ssDNA substrate (5′-AGAAAAGGGGAAAGCAAAGAGGAAAGG-TGAGGAGGT-3′). Measurement and analysis of AID deamination-specific activity were carried out as described (6).

Immunofluorescence—Cells were grown in 35-mm glass bottom microwell dishes (MatTek). After 24 h, cells were stained with 100 ng/ml Hoechst 33342 (Dojindo Laboratories) and then washed to remove unbounded dye. The expression of fluorescent protein was examined by the Biozero fluorescent microscope (BZ-8000) (Keyence) in phenol red-free Dulbecco's modified Eagle's medium (Invitrogen).

Antibodies—Anti-AID mAbs (L7E7 or 30F12, Cell Signaling Technology), anti-GFP rabbit polyclonal Ab (MBL), anti-β-actin Ab (Sigma), anti-FLAG mAb (M2, Sigma), mouse IgG (sc-2025, Santa Cruz Biotechnology, Inc. (Santa Cruz, CA)), rabbit IgG (sc-2027, Santa Cruz Biotechnology, Inc.), anti-GANP (11054-AP, ProteinTech; sc-83297, Santa Cruz Biotechnology), anti-β-tubulin (9F3, Cell Signaling Technology), and anti-histone H3 Ab (catalog no. 9715, Cell Signaling Technology) were purchased.

Preparation of Cytoplasmic and Nuclear Extracts—Splenic B-cells from *ganp*^{Tg} (C57BL/6J-TgN(GANP)meg), *ganp*$^{F/F}$ (Mcm3ap^{tm1Imku}/Mcm3ap^{tm1Imku}), and *CD19-Cre/ganp*$^{F/F}$ (Cd19$^{tm1(cre)Cgn}$/Cd19+ × Mcm3ap^{tm1Imku}/Mcm3ap^{tm1Imku}) mice (20) immunized with sheep red blood cells were isolated after 14 days by using a B-cell isolation kit and an automatic magnetic cell sorter (autoMACS^{TM}) (Miltenyi Biotec). The purified splenic B-cells were stained with Abs to fluoroscein isothiocyanate-conjugated GL7, allophycocyanin-conjugated CD45R/B220, and phycoerythrin-conjugated CD95/Fas (BD Biosciences) (26) and isolated by the JSAN cell sorter system (BayBio Science). Subcellular fractionation was carried out using a subcellular proteome extraction kit (Calbiochem) according to the manufacturer's protocol. The fractionated nuclear and cytoplasmic lysates were verified by Western blotting with anti-β-tubulin and anti-histone H3 Abs. The relative concentration of AID in nuclear fractions was calculated as a normalized ratio of Western blot band intensities of AID to histone H3 using Bio-Rad VersaDoc. All mice were maintained at the Center for Animal Resources and Development, Kuma-

moto University. All studies and procedures were approved by the Kumamoto University Animal Care and Use Committee.

RNA/DNA Chromatin Immunoprecipitation (ChIP) Assay— GFP$^+$ (both GFP alone and GFP-GANP) cells were enriched after transfection of Ramos B-cells with either the *gfp* or *gfp-ganp* cDNA expression vector by cell sorting. Sorted cells were fixed with 1% formaldehyde and incubated for 10 min at room temperature. The cross-linking reaction was quenched with glycine (pH 7.0) at a final concentration of 0.25 M and incubated for 10 min. Cells were harvested by centrifugation at 3,000 × g for 4 min, followed by washing twice with PBS containing a protease inhibitor mixture. Washed cells were lysed in radio-immune precipitation buffer (50 mM Tris-HCl, pH 7.5, 150 mM NaCl, 1 mM EDTA, 1% Nonidet P-40, 0.5% sodium deoxycholate, 0.05% SDS) supplemented with protease inhibitors and were sonicated with three rounds of pulses with 30-s intervals with a Bioruptor™ (Cosmo Bio Corp.). Cell debris was removed by centrifugation at 14,000 rpm for 15 min at 4 °C. An aliquot of clear cell suspension was stored as the input sample (input). The Abs bound to Dynabeads® Protein A or Protein G were used for immunoprecipitation. After 90 min, the beads were washed (six times) with high stringency radioimmune precipitation buffer (50 mM Tris-HCl, pH 7.5, 1 M NaCl, 1 mM EDTA, 1% Nonidet P-40, 1% sodium deoxycholate, 0.1% SDS, 3 M urea). Immunoprecipitated samples were resuspended in elution buffer (50 mM Tris-HCl, pH 7.5, 5 mM EDTA, 10 mM dithiothreitol, and 1% SDS). Reverse cross-linking was performed at 70 °C for 45 min, and the sample was extracted by using TRIzol® reagent (Invitrogen) with chloroform. Aqueous phases were collected and precipitated with Dr. GenTLE™ precipitation carrier (Takara Bio Inc.). After washing with 70% ethanol, samples were resuspended in nuclease-free water, divided into aliquots, and digested either with TURBO DNA-free kit™ for RNA-ChIP or with RNase A (20 μg/ml Nippongene) for DNA-ChIP. After 30 min, samples were subjected with phenol/chloroform/isoamyl alcohol (25:24:1) (Nacalai Tesque), collected by Maxtract low gel (Qiagen), and recovered by ethanol precipitation.

ChIP-qPCR—Real-time qPCR was performed using Applied Biosystems 7500 (Applied Biosystems) and THUNDERBIRD™ SYBR® qPCR Mix (TOYOBO). The IgV$_H$ region was amplified with the primer set of 5′-GACACGTCCAAGAAGCAGC-3′ and 5′-GGCCTAGTAATAACTCTCGC-3′. The *cd4* region was amplified with the primer set of 5′-GGTGGTCAGACTC-GGCTTCCTTCC-3′ and 5′-AGACAACTGGGCAGAGCAC-ATTCCT-3′. The amount of IgV gene was calculated by a standard curve method and normalized to the input.

Sequence Analysis of the IgV$_H$ Gene—The rearranged IgV$_H$ of Ramos cell was amplified with the primer set of 5′-TGGGGC-GCAGGACTGTTGAAGCCTTC-3′ and 5′-CCTTGGCCCC-AGACGTCCAT-3′. The PCR products by PrimeSTAR® HS polymerase (Takara Bio Inc.) were ligated into the pCR4 Zero Blunt® TOPO® sequencing vector (Invitrogen) and then sequenced using ABI3130 Genetic Analyzer with a BigDye™ Terminator (Applied Biosystems).

Statistical Analysis—The statistical significance of differences between two groups was determined using an unpaired two-tailed Student's *t* test. A value of $p < 0.05$ was considered to be of statistical significance.

RESULTS

GANP Binds to AID in Vivo and in Vitro—We examined the physical association of AID and GANP in COS-7 cells by IP-Western blot analysis of cotransfectants with vectors of untagged AID and GFP-GANP. AID is coprecipitated with GFP-GANP, but not with GFP, by the addition of anti-GFP Ab (Fig. 1*A*, *upper gel panel*). The co-IP of AID and GANP is specific because the co-IP by anti-GFP did not contain the nonspecific control β-actin protein (Fig. 1*A*, *upper gel panel*), and the IP with the control IgG did not contain either GANP or AID (Fig. 1*A*, *lower gel panel*). The reciprocal IP with mouse (*M*) monoclonal anti-AID Ab or rabbit (*R*) monoclonal anti-AID Ab confirmed the physical association of AID with GFP-GANP (Fig. 1*B*). The association of AID and GFP-GANP was not affected by treatment with RNase A or DNase I (Fig. 1*C*), suggesting that AID and GANP associate through protein-protein interactions. These results show that AID and GANP form a complex in COS-7 cell nuclei, implying the likelihood that a complex containing GANP and AID may also occur in activated B-cell nuclei. To observe the formation of GANP-AID complex in B-cells, we performed a co-IP analysis for endogenous GANP and AID in Ramos B-cells using monoclonal anti-AID mAb and anti-GANP Ab (Fig. 1*D*). AID was observed with GANP in the IP precipitate by anti-GANP Ab, and, reciprocally, GANP is present in the IP precipitated by anti-AID (*M*) mAb (Fig. 1*D*).

A multiprotein complex involving GANP and AID could of course involve additional proteins. To investigate if GANP and AID are able to interact in the absence of other proteins, FLAG-tagged GANP (FLAG-GANP) and untagged AID were produced *in vitro* using a WGE cell-free system. The FLAG-GANP protein was coprecipitated with AID using anti-AID (*M*) mAb, but not with the control (Fig. 1*E*). A reciprocal IP with anti-FLAG mAb confirms the interaction between AID and GANP, but not with the *in vitro* translated GFP protein (Fig. 1*F*). In agreement with data showing AID-GANP binding in COS-7 cells (Fig. 1*C*), the protein-protein interaction does not appear to involve an RNA or DNA intermediate because it occurs after incubation with RNase A or DNase I (Fig. 1*G*).

A sketch of the AID domain structure is shown in Fig. 2*A*. AID possesses several acidic motifs containing aspartic acid and glutamic acid. Amino acid replacements were made in AID to see if any had a marked effect on co-IP efficiencies *in vitro*. We found that several mutants with a replacement of Glu or Asp with alanine showed reduced binding to GANP (data not shown). One of these mutants, AID (D143A) binds with about a 10-fold lower affinity to GANP compared with WT AID, by densitometric comparison based on co-IP data (Fig. 2*B*). It is important to note that purified AID (D143A) retains significant deamination activity *in vitro* (33% compared with WT AID) (Fig. 2*C*). Thus, although AID (D143A) binds poorly to GANP, it nonetheless retains sufficient structural integrity, enabling it to catalyze significant C deamination *in vitro*.

GANP and AID Colocalize in the Nucleus—We examined the localization of AID in cells in relation to GANP expression. The localization of GANP and AID were visualized in COS-7 cell
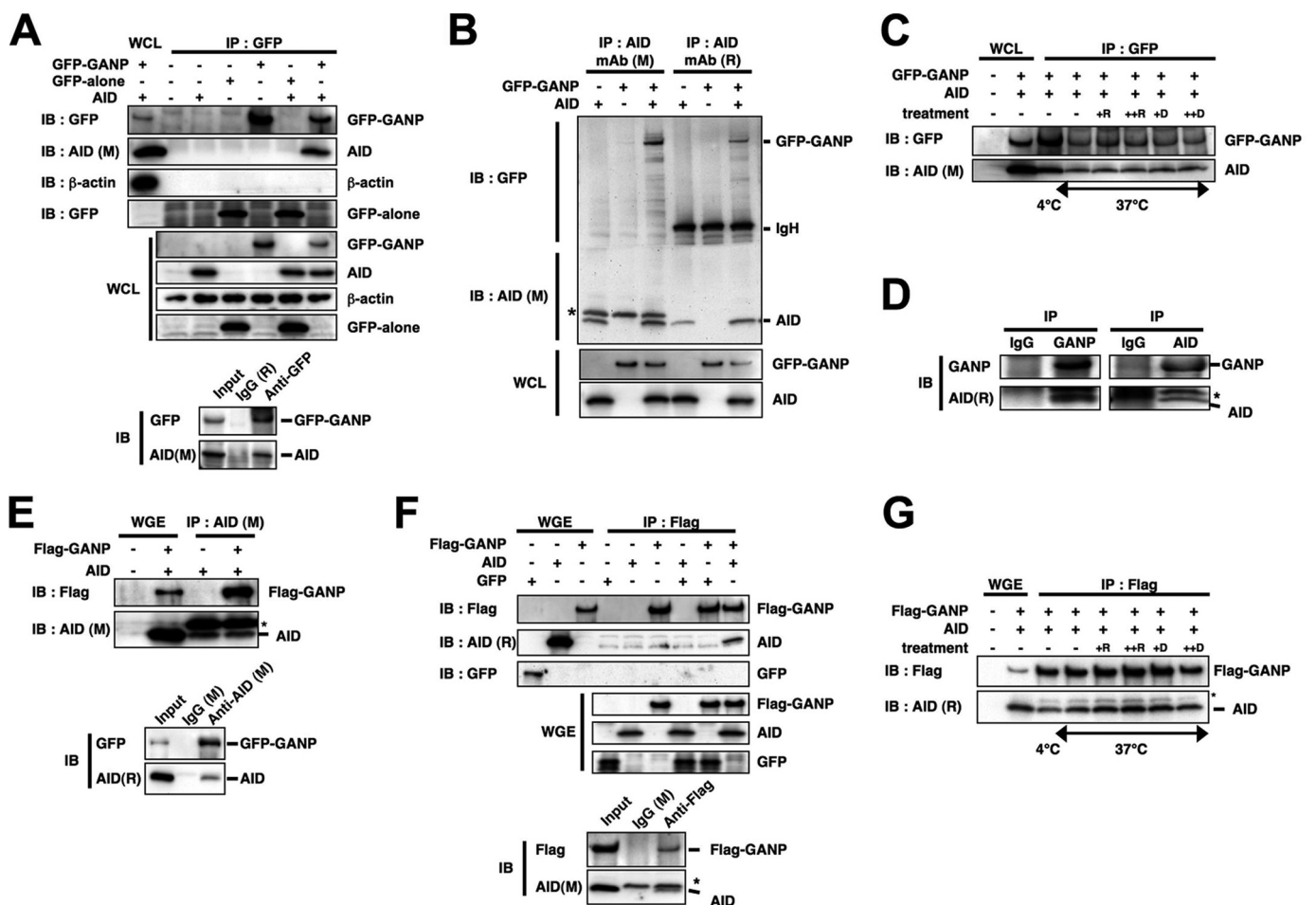
FIGURE 1. **GANP interacts with AID *in vivo* and *in vitro*.** *A*, AID co-IP with GANP. Lysates from COS-7 cells, transfected with GFP-GANP, AID, GFP-GANP + AID, or GFP-alone constructs, were immunoprecipitated using anti-GFP Ab. Immunoblotting (*IB*) was carried out with anti-GFP Ab, anti-AID Ab, or anti-β-actin Ab by IP-Western blot analysis. Specific association in the IP with the anti-GFP Ab was confirmed by comparing with experiments using the control IgG (*bottom panel*). Western blots for whole cell lysates (*WCL*) are shown. *B*, reverse IP-Western blot analysis was performed by IP with anti-AID Abs followed by immunoblot with anti-GFP Ab or anti-AID Ab. The specific signal representing 240-kDa GFP-GANP was detected in immunoprecipitates using both mouse anti-AID Abs (*M mAb*) and rabbit anti-AID Abs (*R mAb*). The anti-AID (M) mAb contains the IgL band (25-kDa) used for IP as indicated with an *asterisk*. *C*, the WCL from COS-7 cells transfected with GFP-GANP and AID constructs was incubated for 10 min with either RNase A (5 μg/ml (+R) or 250 μg/ml (++R)) or DNase I (10 units (+D) or 50 units (++D)) at 4 °C or 37 °C and then immunoprecipitated with anti-GFP Ab followed by immunoblot with anti-GFP or anti-AID (M) Ab. *D*, interaction of endogenous GANP and AID was examined in Ramos B-cells by co-IP. The *asterisk* shows the IgL band. *E* and *F*, FLAG-GANP and AID proteins were synthesized *in vitro* using a WGE cell-free system, and coimmunoprecipitated using anti-AID (M) Ab (*E*) or anti-FLAG Ab (*F*). Controls for specificity of co-IP experiments using mouse (*M*) IgG are shown in the *bottom panels* (*E* and *F*). *G*, the interaction between WGE-produced GANP and AID was still preserved after treatment with RNase A or DNase I. The data were determined from three independent experiments.

transfectants by using constructs of AID fused with red fluorescent protein (DsRed) (AID-DsRed) and GANP fused with GFP (GFP-GANP) (Fig. 3). Transfection of cells with AID-DsRed alone showed that AID is localized mainly in the cytoplasm and is retained in the cytoplasm 40 h post-transfection (Fig. 3, *A* (*left*) and *B*), which agrees with previous data indicating that used immunofluorescence staining and the expression of AID fusion protein (10–12). Transfection of cells with GFP-GANP alone showed that GANP appears in the nucleus and cytoplasm 40 h post-transfection (Fig. 3, *A* and *B*). When AID-DsRed and GFP-GANP were cotransfected, AID predominantly colocalized with GANP in nuclei (Fig. 3*A*, *right*, *Merge*). Among 31 cotransfectants examined, 27 (87%) showed predominant nuclear localization of AID (Fig. 3*B*, *left graph*). As a negative control, we examined localization of a cytoplasmic protein HSP25 fused with DsRed (HSP25-DsRed). HSP25 appears exclusively in the cytoplasm either in the presence or in the

absence of GFP-GANP (Fig. 3, *A* (*lower panel*) and *B* (*left graph*)). These results suggest that GANP specifically interacts with AID and appears to play an important role in relocating AID to the nucleus in B-cells.

To test whether the AID mutant lacking interaction with GANP *in vitro* shows a change in location, we examined the subcellular localization of AID D143A in COS-7 cells. AID (D143A) fused to DsRed appeared exclusively in the cytoplasm in the absence of GFP-GANP, similar to wild type AID (*WT*; Fig. 3, *A* and *B*, *right graph*). Upon coexpression with GANP, the AID mutant showed a dramatic change in the localization (Fig. 3, *A* and *B*). Among 32 AID (D143A) mutant and GFP-GANP cotransfectants, we observed only 3% of cells with predominant nuclear localization of AID and 10% of cells in which AID locates in both cytoplasm and nucleus (Fig. 3*B*, *right graph*). Thus, compared with WT AID (Fig. 3*B*, *left graph*), AID (D143A) appears to lose the ability to relocate to the nucleus in

A

B

C
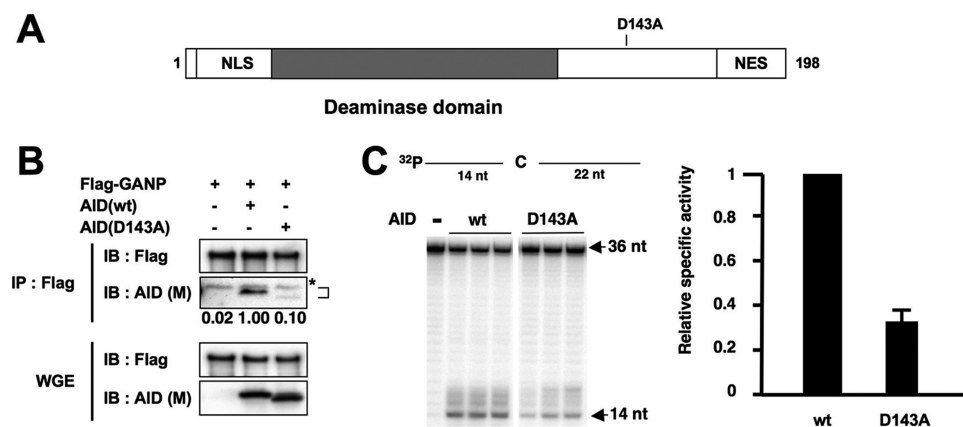
FIGURE 2. **Mutant AID (D143A) binds GANP with significantly reduced affinity compared with wild type AID while retaining substantial C-deamination activity.** *A*, schematic representation of the AID domain structure. *B*, the ability of mutant AID (D143A) to interact with FLAG-GANP was compared with the WT AID by co-IP using anti-FLAG Ab. AID (D143A), AID (WT), and FLAG-GANP were produced using a WGE. The presence of AID in the co-IP precipitate was examined by anti-AID (M) mAb. The *asterisk* shows the IgL band. AID (D143A) migrated slightly faster than WT AID in our gel condition. *C*, deamination activity of AID (WT) and AID (D143A) protein was measured using a ^{32}P-labeled 36-nt ssDNA substrate containing a single C target. ssDNA (30 nM) was incubated with 10 ng of purified *Sf*9-expressed AID (WT or D143A) protein in the presence of RNase A (20 ng) for 5 min at 37 °C. *Left graph*, the deaminated product (14 nt) was separated from the 36-nt substrate by denaturing PAGE and visualized by phosphorimaging. *Right graph*, relative specific activity of mutant AID compared with WT AID. The data were from three independent experiments.

IgV$_H$ Region mRNA and DNA Are Associated with GANP in Ramos B-cells—We examined if GANP and AID could associate specifically with IgV$_H$ region transcripts in Ramos B-cells. GFP-GANP was introduced in Ramos B-cells by transient transfection with a GFP-GANP construct. GFP$^+$ cells were sorted and processed by a modified ChIP assay to identify IgV$_H$ region mRNA in a specific IP (RNA-ChIP; see supplemental Fig. S1). The cells were fixed in formaldehyde, and after treating with DNase I, total RNA bound to GFP-GANP or AID was purified from the IP precipitates with either GFP or AID Ab (see supplemental Fig. S1). IgV$_H$ region mRNA was detected by PCR following reverse transcription using HIV-1 reverse transcription and IgV$_H$-specific primers (Fig. 4*A*). The amplified bands were verified by sequencing. The anti-GFP IP shows a strong IgV$_H$ region mRNA in GFP$^+$ cells containing the GFP-GANP construct, whereas this is not observed in cells transfected with GFP alone (Fig. 4*A*, *IP*: *GFP*). AID binds weakly to IgV$_H$ region mRNA in the absence of GFP-GANP, but AID association is enhanced considerably in cells containing GFP-GANP (Fig. 4*A*, *IP*: *AID*). RNA-ChIP-qPCR of the IgV$_H$ region was performed (Fig. 4, *B* and *D*) to confirm the association of GANP and AID with IgV region mRNA. As a negative control, no IgV$_H$ region mRNA is detected in the IP precipitate with β-actin Ab or with the IgG control in ChIP-qPCR (Fig. 4*B*). The data indicate that GANP and AID associate with IgV$_H$ region mRNA in Ramos B-cells.

We determined if AID and GANP can bind to IgV$_H$ region DNA using ChIP. Genomic DNA was extracted after RNase A treatment from an IP of AID or GFP-GANP (Fig. 4*C*). The presence of the IgV$_H$ region in the IP precipitate with GFP Ab was detected at an elevated level in cells transfected with the GFP-GANP construct but not with the GFP construct alone (Fig. 4*C*), suggesting that GANP binds to the IgV$_H$ region DNA. The use of control β-actin Ab in ChIP-PCR analysis did not show associated IgV$_H$ region DNA. Similar ChIP experiment with AID Ab showed binding of AID to IgV$_H$ region DNA (Fig. 4*C*). The association of IgV$_H$ region DNA with AID is enhanced to a significant extent in Ramos B-cells containing the GFP-GANP construct (Fig. 4*C*), suggesting that GANP may enhance the accessibility of AID to the IgV$_H$ region DNA. We confirmed these results by DNA-ChIP-qPCR (Fig. 4*D*). The use of control IgG in ChIP-qPCR did not show associated IgV$_H$ region DNA. The association of GFP-GANP with the control gene *cd4* was not observed in the ChIPs (Fig. 4*D*). We conclude that GFP-GANP and AID associate with mRNA and genomic DNA of the IgV$_H$ region and that GFP-GANP facilitates AID recruitment to IgV$_H$ region DNA.

the presence of GFP-GANP (Fig. 3*B*, *right graph*). Because AID (D143A) retains a significant activity (Fig. 2*B*) and hence structural integrity, the inability of AID (D143A) to localize in the nucleus probably results from its failure to interact with GANP. These results indicate that specific AID-GANP interactions are needed for efficient transport of AID to the nucleus and that Asp^{143} appears to be an important amino acid residue involved in transport.

We examined AID subcellular localization in GC B-cells from *ganp* mutant mice using *ganp*-deficient (*CD19-Cre/ganp$^{F/F}$*), littermate control (*ganp$^{F/F}$*), and *ganp^{Tg}* mice. Following immunization with sheep red blood cells, GC B-cells (B220$^+$GL7$^+$Fas$^+$) were isolated, and cytoplasmic and nuclear proteins were fractionated. Fractionation efficiency of cytoplasmic and nuclear proteins was verified by the presence of β-tubulin and histone H3 proteins, respectively. The expression of endogenous AID in cytoplasmic or nuclear fraction was detected by Western blotting (Fig. 3*C*, *left gels*). We measured the relative levels of AID in the nuclear fractions by densitometric comparison of Western blot band intensities of AID with control histone H3 as a normalized percentage (Fig. 3*C*, *right graph*). The GC B-cells from GANP-deficient (*CD19-Cre/ganp$^{F/F}$*) mice contained less AID in the nuclear fraction (3.0%) compared with that of control GC B-cells (5.3%) (Fig. 3*C*, *right graph*). In contrast, GC B-cells from *ganp^{Tg}* mice had an increased AID in the nuclear fraction (16.1%) compared with control GC B-cells (5.3%) (Fig. 3*C*, *right graph*). The effect of GANP on AID nuclear localization in GC B-cells is consistent with AID subcellular localization data observed in COS-7 cells (Fig. 3*A*). Taken together, these data suggest that GANP-mediated translocation of AID to the nucleus occurs in GC B-cells and that this process is likely to be important for AID-dependent affinity maturation.
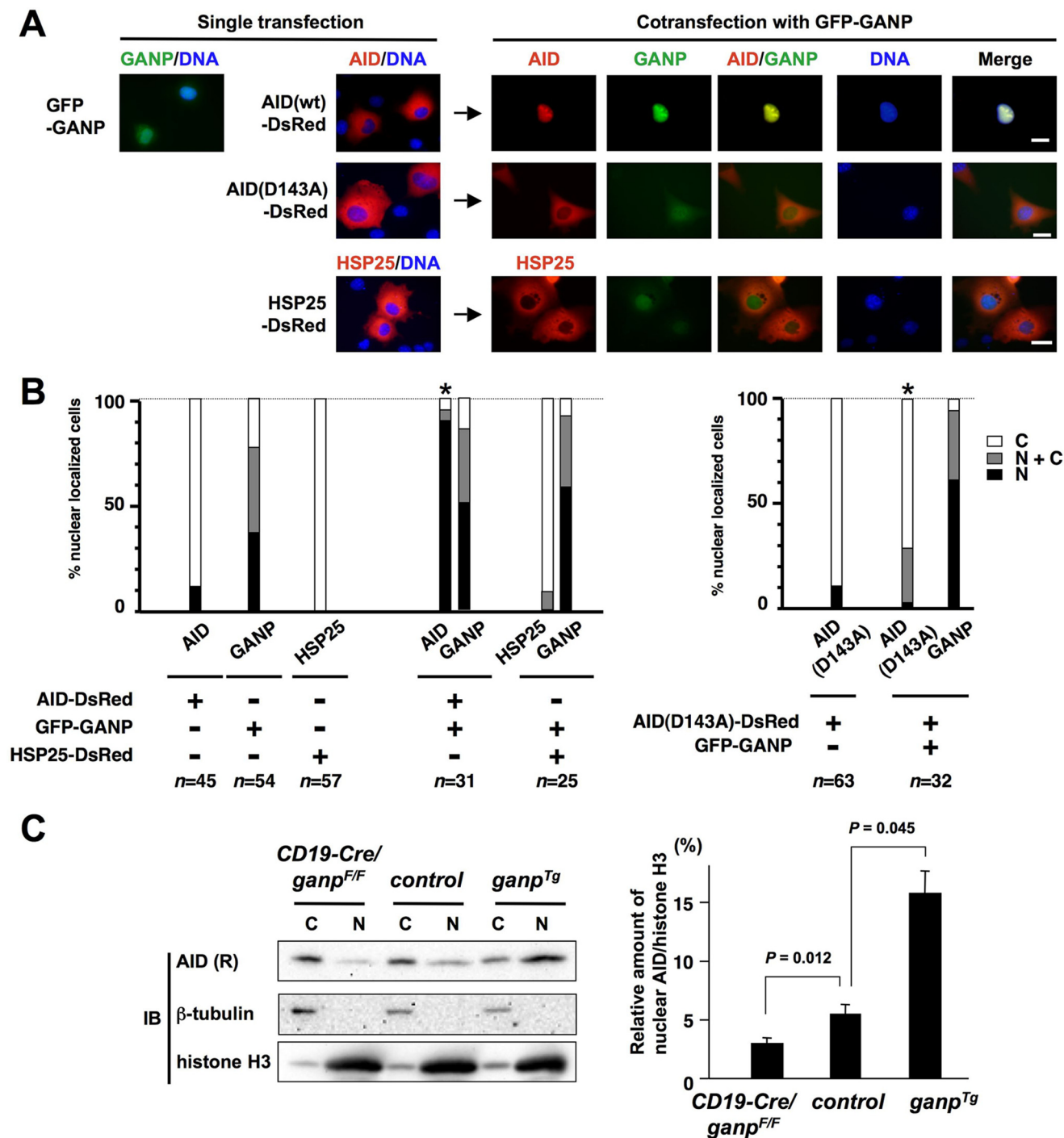
FIGURE 3. **Localization of GANP and AID in COS-7 cells.** *A*, the cells were singly transfected or cotransfected with AID (WT)-DsRed (*top panels*) or AID (D143A)-DsRed (*middle panels*) in combination with GFP-GANP. Transfectants were observed under microscopy for 40 h. As a control, HSP25-DsRed (*bottom panels*) remains strictly cytoplasmic in the absence or presence of coexpressed GFP-GANP. The fluorescence signals were merged with DNA staining after adding Hoechst 33342 in the culture. The *scale bar* represents 20 μm (*right bottom*; *white*) as shown in the *merged pictures*. *B*, subcellular localization of GANP, AID (WT or D143A), and HSP25 was shown by the percentage score as predominantly cytoplasmic (*C*; *white bars*), nuclear (*N*; *black bars*), or in both (*N+C*; *gray bars*) from the indicated number of examined transfected cells (*n*) in multiple microscope fields 40 h after transfection. The significant change (*p* < 0.05) of the nuclear localization of AID (D143A) is marked by an *asterisk*. *C*, nuclear localization of AID in GC B-cell from *ganp*-deficient mice (CD19-Cre/*ganp*[F/F]) and *ganp*[Tg] mice compared with the littermate control (*ganp*[F/F]). Mice (*n* = 3 for each genotype) were immunized with sheep red blood cells, and the splenic GC B-cells (B220[+]GL7^{+}Fas[+]) were isolated by cell sorting. The nuclear (*N*) and cytoplasmic (*C*) fractions were prepared and subjected to Western blotting (*IB*) with anti-AID (R) (rabbit), anti-β-tubulin, and anti-histone H3 Ab (*left gels*). The relative level of AID localized in the nucleus is expressed as a ratio of AID/histone H3 integrated band intensities (*right graph*). The *error bars* (S.E.) and *p* values were determined from three independent experiments.

The IgV$_H$ Region Shows Increased Mutagenesis in the Presence of GANP—Concomitant with an increase in AID access to IgV$_H$ region DNA (Fig. 4C), overexpression of GANP in Ramos B-cells

leads to an increase in IgV$_H$ region SHM. Ramos B-cells containing the GFP-GANP construct have about a 2-fold increase in IgV$_H$ region mutations (1.72×10^{-3}), compared with cells
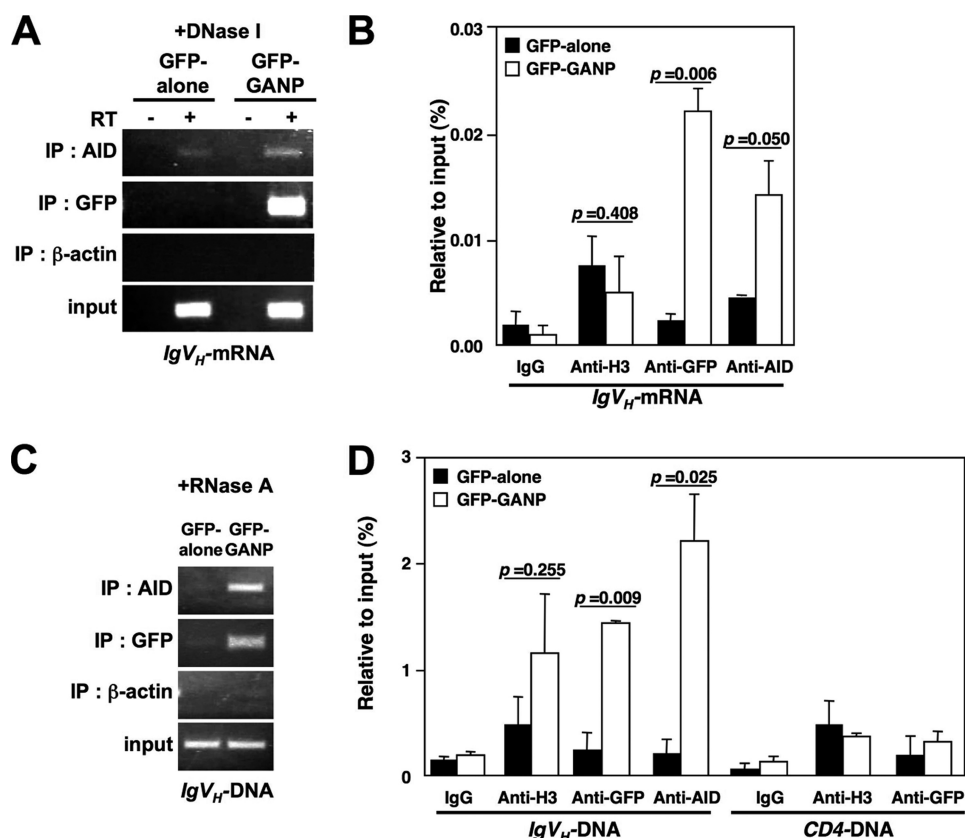
A

+DNase I

B

C

+RNase A

D

FIGURE 4. **Increased GANP expression in Ramos B-cells promotes binding of AID to IgV DNA and mRNA.** *A*, ChIP was used to detect the binding of GANP and AID to IgV_H mRNA. Aliquots of ChIP samples were treated with DNase I for IgV mRNA (RNA-ChIP) and PCR-amplified with specific primers following reverse transcription. *B*, RNA-ChIP-qPCR analysis of Ramos cell transfectants with the GFP-GANP or the GFP-alone control construct. *C*, DNA-ChIP was used to detect the binding of GANP and AID to IgV_H region DNA. Aliquots of ChIP samples were treated with RNase A before PCR amplification with IgV-specific primers. *D*, DNA-ChIP-qPCR analysis for IgV_H region and control *cd4* gene of Ramos cell transfectants with the GFP-GANP or the GFP-alone control construct. *Error bars*, S.E.

TABLE 1

SHM mutation frequency of IgV_H region associated with GANP and AID in Ramos B-cell transfectants

IgV_H region DNA mutations were measured by sequencing of the PCR bands excised from agarose gel electrophoresis shown in Fig. 4*C*. The data were collected from several experiments after transfection of GFP alone or GFP-GANP in Ramos B-cells as shown in supplemental Fig. S1. The mutation frequency was calculated based on comparison with the predetermined sequence of a Ramos B-cell clone. The PCR background mutation frequency is 3×10^{-5}.

	GFP-alone transfectants, input	GFP-GANP transfectants		
		Input	IP with GFP-GANP	IP with AID
No. of sequences	79	87	92	67
Total mutations	23	51	10	43
Mutation frequency ($\times 10^{-3}$)	0.85	1.72^a	0.32	1.89^b

[a] $p < 0.006$.
[b] $p < 2 \times 10^{-7}$.

with a GFP-alone construct (0.85×10^{-3}) (Table 1). To investigate the targeting of AID to the IgV_H region by GANP, we measured SHM in the IgV_H region specifically associated with GANP and AID. We observe an increase (~6-fold) in the mutation frequency of AID-associated IgV_H region DNA (1.89×10^{-3}) compared with GANP-associated IgV_H region DNA (0.32×10^{-3}) (Table 1 and Fig. 5). There is also an increase in the number of mutations per IgV_H region DNA bound with

AID (Fig. 5). Perhaps the lower mutation frequency in the GANP-associated IgV_H region DNA compared with the AID-associated IgV_H region suggests that AID might be recruited after GANP binds to the IgV_H region.

DISCUSSION

SHM and class switch recombination in GC B-cells require the expression of AID, a member of the APOBEC protein family (5, 27). AID predominantly localizes in the cytoplasm (9, 28) and shuttles between nucleus and cytoplasm. Increasing numbers of proteins have recently been implicated in recruiting AID to the nucleus and to help target it to IgV region and/or S region DNA, including RNA polymerase II (13), RPA (8), and CTNNBL-1 (14) and, most recently, protein kinase A (16). GANP can now be added to this list.

Our data show that GANP, a 210-kDa nuclear protein up-regulated in GC B-cells (18–20), facilitates the localization of AID to the nucleus and increases the accessibility of AID to the IgV_H region DNA. Therefore, GANP may be an important, and possibly essential, factor that regulates AID accessibility to IgV_H regions in B-cells. GANP may have several SHM-associated functions. Notably, GANP contains the following DNA interaction domains: an RNA primase region in the N-terminal region (19), similar to DNA primase p49; a MCM3-binding domain (18, 29); and a histone acetyltransferase motif in the C-terminal region (30). The presence of GANP in GC B-cells increases double strand breaks during transcription of the IgV_H region (26), suggesting a role in DNA repair. A midregion of GANP shows a moderate degree of homology to *Saccharomyces* Sac3, suggested to be part of an RNA export complex (22). The loss of Sac3 in yeast causes retardation of cell cycle progression accompanied by transcription-coupled DNA hyperrecombination (21).

We found that SHM is increased in Ramos B-cells when GANP is expressed ectopically (Table 1). We have identified an important AID amino acid residue (Asp[143]) needed for interaction with GANP. Mutant AID (D143A) binds with ~10-fold lower affinity to GANP *in vitro* (Fig. 2*A*) and prohibits nuclear relocalization of AID when coexpressed with GANP (Fig. 3), yet this mutant retains significant deamination activity (Fig. 2*B*), suggesting that its inability to interact with GANP is probably not caused by a loss in structural integrity. Instead, we suggest that the Asp[146] residue is needed for association and colocalization with GANP in the nucleus.
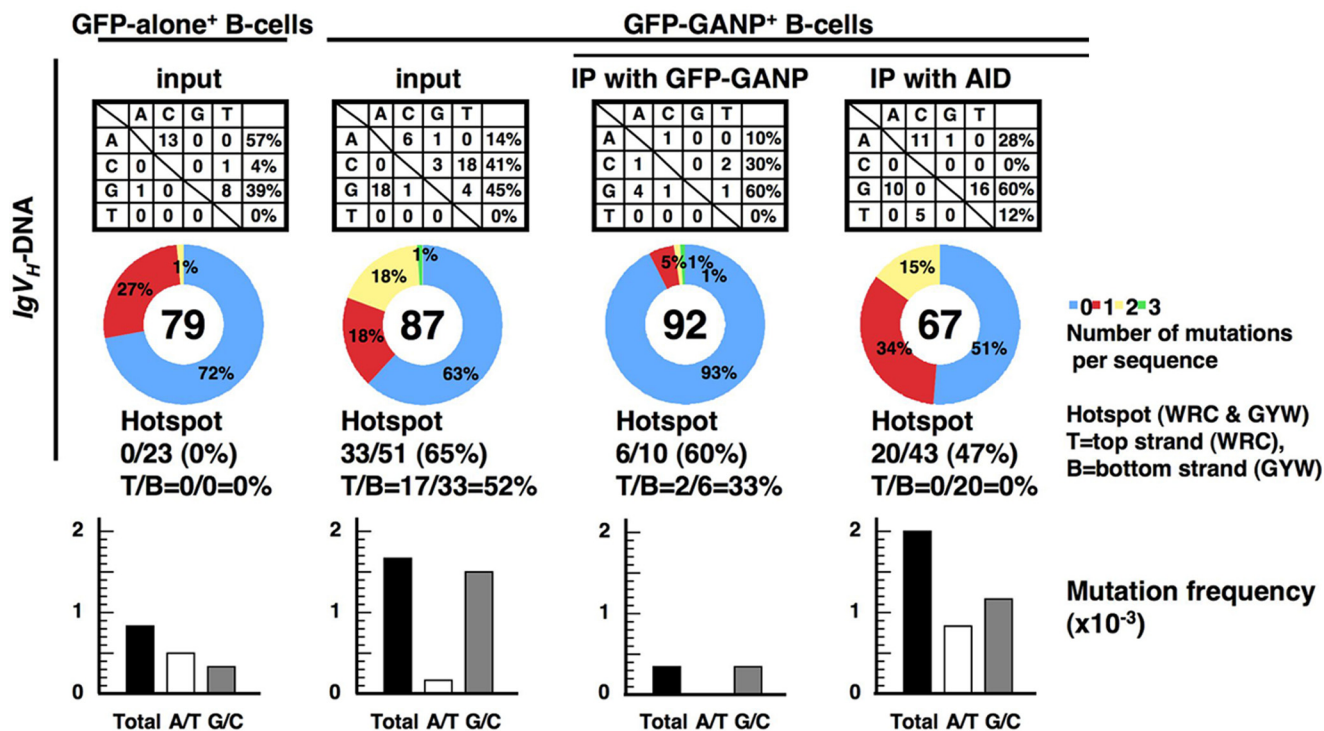
FIGURE 5. **Mutation analysis of SHM of IgV$_H$ region gene in Ramos B-cells transfected with *gfp* alone or *gfp-ganp* constructs.** The patterns of nucleotide substitutions in the genomic IgV$_H$ region of GFP and GFP-GANP transfectants are shown (*input*). For GFP-GANP transfectants, IgV$_H$ region DNA, associated with GFP-GANP or AID, was isolated from IP precipitates using anti-GFP Ab or anti-AID Ab and sequenced. The *number* in the *center* of the *pie chart* indicates the number of IgV$_H$ region sequences analyzed, and the *color* of each *part* of the *pie* indicates the mutation number of each sequence as 0 (*blue*), 1 (*red*), 2 (*yellow*), and 3 (*green*). The percentage frequencies are shown. The mutation frequency at WRC hot spots (WRC and GYW) was counted and estimated for the top and bottom strands.
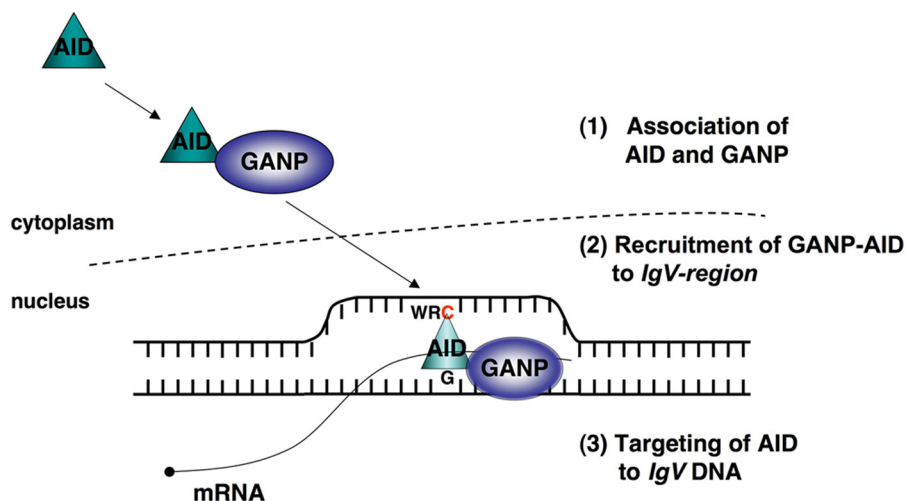

FIGURE 6. **A model of AID targeting by GANP.** AID and GANP are induced in GC B-cells. AID is abundant in the cytoplasm and becomes localized at the nucleus in the presence of cofactors, including GANP. The observation that GANP binds to IgV DNA and RNA and to AID and that the binding of AID to IgV DNA is enhanced in the presence of GANP, accompanied by a 6-fold increase in SHM, suggests that GANP plays an important role in targeting AID to actively transcribed IgV DNA.

The observed effect of GANP protein on AID localization in GC B-cells, a decrease in AID nuclear localization in *ganp*-deficient mice and an increase in nuclear localization in GANP transgenic mice (Fig. 3C), suggests that GANP-dependent relocation of AID to the nucleus occurs in GC B-cells and that it may play an important role in Ig affinity maturation. The ability of GANP to facilitate the targeting of AID to the nucleus and IgV$_H$ region DNA helps to explain previous observations

that showed that GANP enhances affinity maturation of Abs against T-cell-dependent Ags, accompanied by increased mutation frequencies at the IgV$_H$ regions in mutant *ganp^{Tg}* mice (25). GANP is required for high affinity Ab maturation *in vivo* (20, 25). The loss of GANP results in decreased production of high affinity Abs against nitrophenyl (NP)-chicken γ-globulin, with decreased SHM at IgV$_{H186.2}$ (20). Conversely, *ganp^{Tg}* mice, which overexpress GANP, produced much higher affinity Abs against Ags accompanied by increased mutations, compared with WT C57BL/6 mice (25). The *ganp^{Tg}* mice introduced changes of more than 15 amino acids at the non-canonical IgV$_H$ region, IgV$_{H7183}$, and generated the mAbs against nitrophenyl-hapten with high affinities ($K_D > 1.57 \times 10^{-9}$ M) similar to that of the canonical anti-NP mAb of the IgV$_H$ region, IgV$_{H186.2}$, mutated at tryptophan 33 to leucine in C57BL/6 mice (25).

Our data suggest a dual functional role for GANP in SHM. GANP is involved in transporting AID from the cytoplasm to the B-cell nuclei. Then, via its association with IgV$_H$ region DNA and RNA and with AID, GANP may help to target AID to

specific regions undergoing transcription, including IgV and various genes (17). A sketch depicting these possible roles for GANP is shown in Fig. 6. We speculate that GANP could in principal help to target AID to transcribed IgV$_H$ region DNA. Increased AID targeting could be achieved by direct recruitment through interaction with GANP and by GANP-mediated enhanced IgV transcription. Our data showing that GANP and AID bind to IgV$_H$ DNA and RNA suggest the possibility that binding could be occurring to a transcription bubble. The action of AID during transcription is necessary for SHM (17). Interactions between GANP and AID as observed here are consistent with the observation that *ganp*^{Tg} mice generate exceptionally high affinity monoclonal Abs against nitrophenyl-hapten, HIV(V3)-epitope (25), and SARS-CoV-epitope ($K_D >$ 10^{-11} M). These mice develop Hodgkin-like lymphomas of non-T and non-B surface phenotype with multiple mutations at IgV$_H$ region genes (31). More generally, our data suggest a means by which AID is recruited from the cytoplasm to the nucleus and is then able to bind to IgV$_H$ region DNA to initiate SHM required for Ig diversification in B-cells.

REFERENCES

1. MacLennan, I. C. (1994) *Annu. Rev. Immunol.* **12,** 117–139
2. Rajewsky, K. (1996) *Nature* **381,** 751–758
3. Muramatsu, M., Kinoshita, K., Fagarasan, S., Yamada, S., Shinkai, Y., and Honjo, T. (2000) *Cell* **102,** 553–563
4. Di Noia, J. M., and Neuberger, M. S. (2007) *Annu. Rev. Biochem.* **76,** 1–22
5. Peled, J. U., Kuang, F. L., Iglesias-Ussel, M. D., Roa, S., Kalis, S. L., Goodman, M. F., and Scharff, M. D. (2008) *Annu. Rev. Immunol.* **26,** 481–511
6. Bransteitter, R., Pham, P., Scharff, M. D., and Goodman, M. F. (2003) *Proc. Natl. Acad. Sci. U.S.A.* **100,** 4102–4107
7. Pham, P., Bransteitter, R., Petruska, J., and Goodman, M. F. (2003) *Nature* **424,** 103–107
8. Chaudhuri, J., Khuong, C., and Alt, F. W. (2004) *Nature* **430,** 992–998
9. Pasqualucci, L., Guglielmino, R., Houldsworth, J., Mohr, J., Aoufouchi, S., Polakiewicz, R., Chaganti, R. S., and Dalla-Favera, R. (2004) *Blood* **104,** 3318–3325
10. Rada, C., Jarvis, J. M., and Milstein, C. (2002) *Proc. Natl. Acad. Sci. U.S.A.* **99,** 7003–7008
11. McBride, K. M., Barreto, V., Ramiro, A. R., Stavropoulos, P., and Nussenzweig, M. C. (2004) *J. Exp. Med.* **199,** 1235–1244
12. Ito, S., Nagaoka, H., Shinkura, R., Begum, N., Muramatsu, M., Nakata, M., and Honjo, T. (2004) *Proc. Natl. Acad. Sci. U.S.A.* **101,** 1975–1980
13. Nambu, Y., Sugai, M., Gonda, H., Lee, C. G., Katakai, T., Agata, Y., Yokota, Y., and Shimizu, A. (2003) *Science* **302,** 2137–2140
14. Conticello, S. G., Ganesh, K., Xue, K., Lu, M., Rada, C., and Neuberger, M. S. (2008) *Mol. Cell* **31,** 474–484
15. Basu, U., Chaudhuri, J., Alpert, C., Dutt, S., Ranganath, S., Li, G., Schrum, J. P., Manis, J. P., and Alt, F. W. (2005) *Nature* **438,** 508–511
16. Vuong, B. Q., Lee, M., Kabir, S., Irimia, C., Macchiarulo, S., McKnight, G. S., and Chaudhuri, J. (2009) *Nat. Immunol.* **10,** 420–426
17. Liu, M., Duke, J. L., Richter, D. J., Vinuesa, C. G., Goodnow, C. C., Kleinstein, S. H., and Schatz, D. G. (2008) *Nature* **451,** 841–845
18. Kuwahara, K., Yoshida, M., Kondo, E., Sakata, A., Watanabe, Y., Abe, E., Kouno, Y., Tomiyasu, S., Fujimura, S., Tokuhisa, T., Kimura, H., Ezaki, T., and Sakaguchi, N. (2000) *Blood* **95,** 2321–2328
19. Kuwahara, K., Tomiyasu, S., Fujimura, S., Nomura, K., Xing, Y., Nishiyama, N., Ogawa, M., Imajoh-Ohmi, S., Izuta, S., and Sakaguchi, N. (2001) *Proc. Natl. Acad. Sci. U.S.A.* **98,** 10279–10283
20. Kuwahara, K., Fujimura, S., Takahashi, Y., Nakagata, N., Takemori, T., Aizawa, S., and Sakaguchi, N. (2004) *Proc. Natl. Acad. Sci. U.S.A.* **101,** 1010–1015
21. Gallardo, M., Luna, R., Erdjument-Bromage, H., Tempst, P., and Aguilera, A. (2003) *J. Biol. Chem.* **278,** 24225–24232
22. Fischer, T., Strässer, K., Rácz, A., Rodriguez-Navarro, S., Oppizzi, M., Ihrig, P., Lechner, J., and Hurt, E. (2002) *EMBO J.* **21,** 5843–5852
23. Köhler, A., and Hurt, E. (2007) *Nat. Rev. Mol. Cell Biol.* **8,** 761–773
24. Osman, W., Laine, S., and Zilliacus, J. (2006) *Biochem. Biophys. Res. Commun.* **348,** 1239–1244
25. Sakaguchi, N., Kimura, T., Matsushita, S., Fujimura, S., Shibata, J., Araki, M., Sakamoto, T., Minoda, C., and Kuwahara, K. (2005) *J. Immunol.* **174,** 4485–4494
26. Kawatani, Y., Igarashi, H., Matsui, T., Kuwahara, K., Fujimura, S., Okamoto, N., Takagi, K., and Sakaguchi, N. (2005) *J. Immunol.* **175,** 5615–5618
27. Stavnezer, J., Guikema, J. E., and Schrader, C. E. (2008) *Annu. Rev. Immunol.* **26,** 261–292
28. Patenaude, A. M., Orthwein, A., Hu, Y., Campo, V. A., Kavli, B., Buschiazzo, A., and Di Noia, J. M. (2009) *Nat. Struct. Mol. Biol.* **16,** 517–527
29. Takei, Y., and Tsujimoto, G. (1998) *J. Biol. Chem.* **273,** 22177–22180
30. Takei, Y., Swietlik, M., Tanoue, A., Tsujimoto, G., Kouzarides, T., and Laskey, R. (2001) *EMBO Rep.* **2,** 119–123
31. Fujimura, S., Xing, Y., Takeya, M., Yamashita, Y., Ohshima, K., Kuwahara, K., and Sakaguchi, N. (2005) *Cancer Res.* **65,** 5925–5934